FULL PAPER

BJC

British Journal of Cancer (2015) 113, 252–258 | doi: 10.1038/bjc.2015.170

Keywords: microRNA; Hippo pathway; TAZ; hepatocellular carcinoma

miR-9-3p plays a tumour-suppressor role by targeting TAZ (WWTR1) in hepatocellular carcinoma cells

T Higashi[1], H Hayashi[1], T Ishimoto[1], H Takeyama[1], T Kaida[1], K Arima[1], K Taki[1], K Sakamoto[1], H Kuroki[1], H Okabe[1], H Nitta[1], D Hashimoto[1], A Chikamoto[1], T Beppu[1] and H Baba*[,1]

[1]*Department of Gastroenterological Surgery, Graduate School of Medical Science, Kumamoto University, 1-1-1 Honjo, Kumamoto 860-8556, Japan*

Background: The inactivation of the Hippo pathway lead to TAZ (PDZ-binding motif)/YAP (yes-associated protein) overexpression, and is associated with worse prognostic outcomes in various cancers including hepatocellular carcinoma (HCC). Although there are several reports of microRNA (miR) targeting for YAP, miR targeting for TAZ remains unclear. The aim of this study is to identify the miR targeting TAZ expression in HCC.

Methods: MicroRNA expression was analysed using the Human miFinder 384HC miScript miR PCR array, and was compared between low and high TAZ expression cell lines. Then, we extracted miR-9-3p as a tumour-suppressor miR targeting TAZ. We examined the functional role of miR-9-3p using miR-9-3p mimic and inhibitor in HCC cell lines).

Results: In HCC cell lines and HCC clinical samples, there was the inverse correlation between miR-9-3p and TAZ expressions. TAZ expression was induced by treatment of miR-9-3p inhibitor and was downregulated by treatment of miR-9-3p mimic. Treatment of miR-9-3p mimic inhibited cell proliferative ability with downregulated phosphorylations of Erk1/2, AKT, and β-catenin in HLF. Inversely, treatment of miR-9-3p inhibitor accelerated cell growth compared with control in HuH1.

Conclusions: MicroRNA-9-3p was identified as the tumour-suppressor miR targetting TAZ expression in HCC cells.

Hepatocellular carcinoma (HCC) is the sixth most prevalent cancer and the third most frequent cause of cancer-related death (Forner *et al*, 2012). Despite recent advances in cancer treatment including the development of molecular-targeted drugs, the prognosis of patients with HCC remains poor. In 2003, the Hippo pathway was identified as a novel signalling cascade that controls organ size by inhibiting cell proliferation and promoting apoptosis (Wu *et al*, 2003; Ramos and Camargo, 2012). Defects in the Hippo pathway induce the hyperactivation of its downstream effectors such as transcriptional co-activator with PDZ-binding motif (TAZ) and yes-associated protein (YAP) (Qin *et al*, 2013); their overexpression is often detectable and is associated with worse prognostic outcome in various cancers including HCC (Zhao *et al*, 2007; Xu *et al*, 2009; Liu *et al*, 2010b; Zhao *et al*, 2012; Huo *et al*, 2013; Yuen *et al*, 2013; Bartucci *et al*, 2014; Han *et al*, 2014; Ma *et al*, 2014), suggesting that TAZ and YAP could be novel therapeutic targets.

MicroRNAs (miRs) are small non-coding RNAs that repress the translation of their target mRNAs by base pairing to partially complementary sequences in their 3′-untranslated region (UTR). MicroRNAs have important regulatory functions in processes such as differentiation, proliferation, and inhibiting apoptosis (Chen *et al*, 2004; Croce and Calin, 2005), and regulate the expression of many target genes, and dysregulation of miRs are associated with various cancers. Although there are some reports of miR targeting of YAP, such as miR-375 (Liu *et al*, 2010a), -135b (Lin *et al*, 2013), -29 (Tumaneng *et al*, 2012), and -let7 (Chen *et al*, 2012), there are no reports of miR targeting of TAZ. The aim of this study was to identify the miR that controls TAZ expression in HCC.

*Correspondence: Dr H Baba; E-mail: hdobaba@kumamoto-u.ac.jp

Received 7 February 2015; revised 17 March 2015; accepted 14 April 2015; published online 30 June 2015

MATERIALS AND METHODS

Cell lines and culture. Established HCC cell lines (HepG2, HuH1, HuH7, HLE, HLF, PLC, and SKHep1) were used in the current study. These cell lines were obtained from the Japanese Collection of Research Bioresources Cell Bank and Riken BioResource Center Cell Bank. All lines were cultured under 5% CO_2 at 37 °C in Dulbecco's modified Eagle's medium (Wako, Osaka, Japan) supplemented with 10% fetal bovine serum (FBS). All cultures were maintained in a 5% CO_2 air-humidified atmosphere at 37 °C.

RNA and miRNA isolation. Total RNA was isolated from cell lines and frozen tissues using a miRNeasy Mini Kits (Qiagen, Valencia, CA, USA) and finally eluted into 30 μl of heated elution solution, according to the manufacturer's protocol. The purity and concentration of all RNA samples was evaluated by their absorbance ratio at 260/280 nm, determined using a NanoDrop ND-1000 spectrophotometer (NanoDrop Technologies, Rockland, DE, USA).

MicroRNA PCR array. MicroRNA expression was analysed using the Human miFinder 384HC miScript miRNA PCR Array (Qiagen; MIHS-3001Z), which profiles the expression of the 372 most abundantly expressed and best-characterised miRNAs in miRBase, according to the manufacturer's instructions.

Luciferase assays. HLF cells in 96-well plates were transfected with pmirGLO Dual-Luciferase miRNA Target Expression Vector (Promega, Tokyo, Japan: E1330) containing firefly luciferase and renilla luciferase, and Luc-TAZ-a, aM, b, bM, or control (non-insert), and mimic negative control (NC) or mimic miR-9-3p (Invitrogen, Carlsbad, CA, USA) using MultiFectam (Promega: ETF5000). Reporter assays were performed at 48 h after transfection, and firefly and renilla luciferase activities were measured using the Dual-Glo Luciferase Assay System (Promega: E2940). All transfection experiments were conducted in triplicate.

Quantitative real-time reverse transcription PCR. The expression levels of miR-9-3p were determined by quantitative real-time reverse transcription PCR (qRT–PCR) using TaqMan MicroRNA Assay Kits (Applied Biosystems, Foster City, CA, USA). For synthesis of cDNA, 10 ng of total RNA for each serum sample was used for individual assays in a 15-μl reaction mixture containing 5 μl RNA extract, 0.15 μl of 100 mM dNTPs, 1 μl multiscribe reverse transcriptase (50 U ml^{-1}), 1.5 μl of 109 reverse transcription buffer, 0.19 μl RNase inhibitor (20 U ml^{-1}), 1 μl gene-specific TaqMan primer (Supplementary Table 1), and 4.16 μl nuclease-free water. *TAZ* expression levels were quantified by SYBR Green qRT–PCR using a LightCycler 480 SYBR Green I Master (Roche Diagnostics, Mannheim, Germany) and normalised to *ACTB* (β-actin). The reaction mixture was incubated at 16 °C for 30 min, 42 °C for 60 min, and 85 °C for 5 min. Subsequently, 5 μl cDNA template was amplified using 10 μl LightCycler 480 SYBR Green I Master (Roche Diagnostics), 3 μl of nuclease-free water, and 2 μl gene-specific primers (Supplementary Table 1) mix in a final volume of 20 μl. Quantitative RT–PCR was run on a LightCycler 480 System II (Roche Diagnostics). The reaction mixture was incubated at 95 °C for 5 min, followed by 40 cycles of 95 °C for 10 s, 60 °C for 30 s, and 72 °C for 1 s. All qRT–PCRs were run using the LightCycler 480 System II (Roche Diagnostics). The relative amounts of miR-9-3p and *TAZ* were measured with the $2-\Delta\Delta CT$ method. All qRT–PCRs were performed in triplicate.

MicroRNA transfection. Cells were transfected with 20 nM miR-9-3p mimic or inhibitor (Applied Biosystems) using Lipofectamine 2000 or RNAiMax transfection reagent (Invitrogen), according to the manufacturer's instructions. The specificity of the transfection was verified using a NC mimic (Applied Biosystems). The expression levels of miR-9-3p were quantified 48 h after transfection, and the cells were used for subsequent experiments.

Western blot analysis. To isolate the proteins, cells collected from six-well plates were washed once in phosphate-buffered saline and lysed in RIPA buffer. Each protein sample (12 μg) was resolved by SDS–polyacrylamide gel electrophoresis, transferred onto polyvinylidene difluoride membranes, and incubated with monoclonal antibodies, as follows: TAZ/YAP (1:1000; Cell Signaling, Danvers, MA, USA), N-cadherin (1:1000; clone 56, BD Biosciences, Tokyo, Japan), E-cadherin (1:1000; Cell Signaling), phosphorylated-AKT (p-AKT; 1:1000; Cell Signaling), AKT (1:1000; Cell Signaling), phosphorylated-ERK1/2 (p-ERK1/2; 1:1000; Cell Signaling), ERK1/2 (1:1000; Cell Signaling), phosphorylated β-catenin (p-β-catenin; 1:1000; Cell Signaling), β-catenin (1:1000; Cell Signaling), β-actin (1:2000; Cell Signaling), α-tubulin (1:20 000; Abcam, Cambridge, MA, USA), or histone H3 (1:20 000; Abcam). The signals were detected by incubation with secondary antibodies labelled with the ECL Detection System (GE Healthcare, Little Chalfont, UK).

Cell fractionation. To prepare cytoplasmic and nuclear extracts for western blotting, transfected cell pellets were resuspended in hypotonic buffer (20 mM HEPES (pH 8.0), 10 mM KCl, 1 mM $MgCl_2$, 0.1% Triton X-100, and 20% glycerol) and incubated on ice for 10 min. Cytoplasmic fractions were obtained by collecting supernatants following centrifugation at 1500 **g** for 5 min. Pellets were washed twice in hypotonic buffer, centrifuged at 5000 **g** for 5 min, and lysed on ice for 1 h in RIPA buffer (50 mM Tris (pH 7.5) 150 mM NaCl, 0.1% SDS, 0.5% sodium deoxycholate, and 1% NP40) followed by centrifugation at 21 000 **g** for 10 min. All buffers were supplemented with complete protease inhibitor cocktail (Thermo Scientific, Waltham, MA, USA).

Invasion assay. Biocoat Matrigel-coated invasion chambers (BD Biosciences, San Jose, CA, USA) were used to examine cell invasion. In brief, 1.0×10^5 HLF and 1.5×10^5 HuH1 cells in 500 μl serum-free medium were added to the upper chamber. Medium containing 10% FBS was added to the lower chamber. The cells were allowed to invade the Matrigel for 24 h at 37 °C in 5% CO_2 atmosphere. After 22 h, the non-invading cells were removed with a cotton swab, and the invading cells were stained with 1% toluidine blue and counted under a microscope at $\times 20$ magnification.

Proliferation assay. Cells were seeded in a 96-well plate at a density of 2000 cells per well. The medium in each well was changed daily. Viable cell numbers were measured with a Cell Counting Kit-8 containing 2-(2-methoxy-4-nitrophenyl)-3-(4-nitrophenyl)-5-(2,4-disulfophenyl)-2H-tetrazolium (WST-8; Dojin Laboratories, Kumamoto, Japan) for 0, 24, 48, 72, and 96 h, according to the manufacturer's instructions. Optical density (450 nm) was measured using an automatic microplate reader (Molecular Devices, Osaka, Japan). Each experiment was performed in triplicate.

Clinical samples. Frozen HCC tissue was obtained from patients who had undergone hepatic resection. The study was approved by the Medical Ethics Committee of Kumamoto University, and written informed consent was obtained from the human subjects.

Statistical analysis. Statistical analyses were performed using the JMP programme (SAS Institute, Cary, NC, USA). Quantitative data were expressed as mean ± s.d., unless otherwise stated. The χ^2-test was used to analyse relationships between categorical variables. $P < 0.05$ was considered significant.

RESULTS

Identification of miRs regulating TAZ expression using cancer-related miR screening in HCC cell lines. We first examined the expression profile of TAZ/YAP by western blotting in seven HCC cell lines (HepG2, HuH1, HuH7, HLE, HLF, PLC, and SKHep1). TAZ protein was the predominant expression profile in HCC cell lines (Figure 1A). By qRT–PCR, HepG2, HLE, and HLF revealed high *TAZ* mRNA levels, whereas HuH1, PLC, and SKHep1 expressed low levels (Figure 1B). To identify the miRs that regulate *TAZ* expression, miR qRT–PCR array analysis was performed to compare the high TAZ-expressing cell lines (HepG2, HLE, and HLF) and the low TAZ-expressing cell lines (HuH1, PLC, and SKHep1). Twenty-four miRs showed low expression in high TAZ-expressing cells by less than three-fold compared with the low TAZ-expressing cell group (Table 1). In addition, 133 miRs were highlighted as candidates that directly target human TAZ 3′-UTR using online databases (miRTarBase, TarBase, microRNA.org, and TargetScanHuman). Finally, miR-9-3p was extracted as a candidate that met both requirements (Figure 1C).

TAZ as a direct binding target of miR-9-3p. Next, using luciferase reporter assays, we confirmed whether miR-9-3p targeted the 3′-UTR of TAZ mRNA. The predicted target sequence of miR-9-3p in the TAZ 3′-UTR was checked using the miRanda algorithm. Luc-TAZ-a and -b represent alignments of the predicted miR-9-3p target sequences in the wild-type TAZ 3′-UTR mRNA. Seed sequences are indicated by lines in Figure 2A. HLF cells transfected with a miR-9-3p mimic significantly suppressed luciferase activity from the reporter vectors containing Luc-TAZ-a but not Luc-TAZ-b compared with the control vectors ($P<0.001$; Figure 2B). We also constructed reporter vectors containing the mutated TAZ 3′-UTR (Luc-TAZ-aM and Luc-TAZ-bM). HLF cells transfected with a miR-9-3p mimic failed to suppress luciferase activity from the reporter vectors containing the mutated 3′-UTR of TAZ compared with the wild-type 3′-UTR-containing vector (Figure 2B). These results indicated that miR-9-3p regulated TAZ expression by directly targeting its 3′-UTR.

We investigated whether miR-9-3p successfully modulated TAZ protein expression in HLF cells with high TAZ expression and HuH1 cells with low TAZ expression. HLF cells transfected with miR-9-3p mimic showed decreased TAZ protein levels, whereas HuH1 cells treated with miR-9-3p inhibitor displayed increased TAZ protein levels in comparison with the controls (Figure 2C). TAZ nuclear localisation was indeed inhibited with miR-9-3p mimic treatment in HLF cells, and was upregulated by miR-9-3p inhibitor treatment in HuH1 cells (Figure 2D). In 55 human HCC tissues, we examined miR-9-3p and *TAZ* expression levels using qRT–PCR. We divided them into two subgroups according to their miR-9-3p expression (low vs. high) based on the median value. Cancer tissues with high miR-9-3p expression displayed significantly lower *TAZ* mRNA levels compared with those exhibiting high miR-9-3p expression ($P=0.016$; Figure 3A). There was an inverse correlation between miR-9-3p and *TAZ* mRNA expression in HCC cell lines (Figure 3B).

miR-9-3p promotes cancer cell proliferation but not invasiveness by modulating AKT, ERK1/2, and β-catenin signalling. We examined the functional relevance of miR-9-3p expression in cancer cells. HLF cells transfected with miR-9-3p mimic showed significantly reduced cell proliferation compared with the control

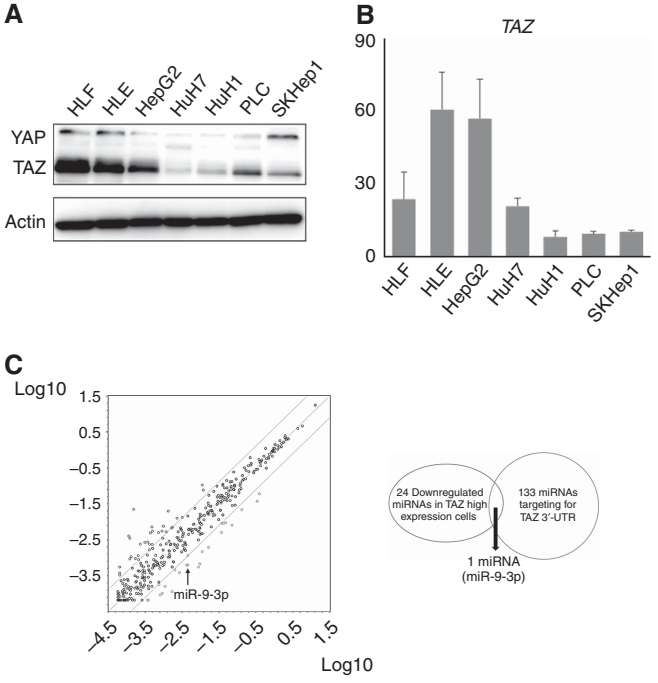

Figure 1. Identification of miRs regulating TAZ expression via cancer-related miR screening in HCC cell lines. (**A** and **B**) TAZ and YAP expression in seven HCC cell lines by qRT–PCR and western blot analysis. (**C**) Analysis of the Human miFinder 384HC miScript miRNA PCR Array. Twenty-four miRs showed low expression by less than three-fold in high TAZ-expressing cells (HepG2, HLE, and HLF) compared with low TAZ-expressing cells (HuH1, PLC, and SKHep1). Of 133 miRs that were highlighted as candidates directly targeting the human TAZ 3′-UTR using online databases, miR-9-3p directly targeted TAZ.

Table 1. MicroRNAs lists showing low expression in high TAZ-expressing cell group with less than three-fold compared with low TAZ-expressing cell group

miRs	Folds change
let-7b-5p	4.6
miR-122-5p	15.7
miR-122-3p	6.9
miR-126-3p	8.9
miR-126-5p	8.6
miR-135a-5p	7.6
miR-135b-5p	4.0
miR-149-5p	4.2
miR-155-5p	5.8
miR-182-3p	4.2
miR-192-5p	9.4
miR-192-3p	7.1
miR-194-5p	6.5
miR-196a-5p	5.1
miR-196b-5p	14.2
miR-203a	5.6
miR-208a	8.8
miR-215	7.3
miR-218-1-3p	9.3
miR-34a-3p	4.4
miR-424-5p	6.0
miR-551b-3p	15.1
miR-9-5p	7.5
miR-9-3p	6.8

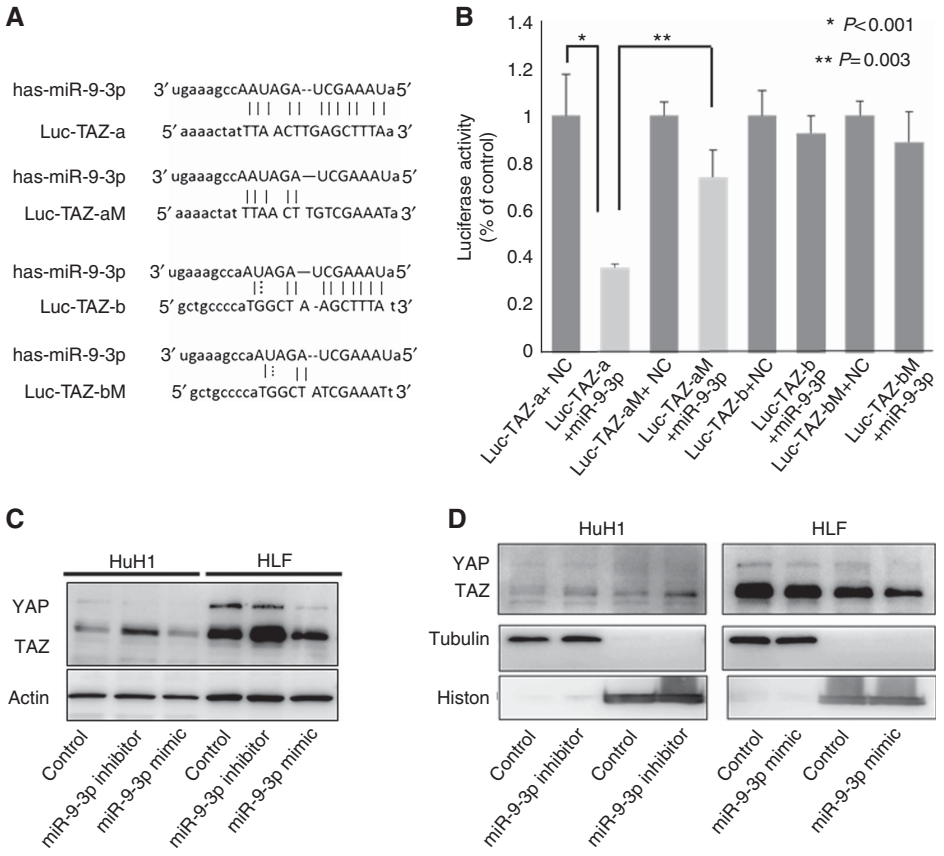

Figure 2. TAZ as a direct binding target of miR-9-3p. (**A**) The predicted target sequence of miR-9-3p in the TAZ 3′-UTR. (**B**) Luciferase reporter assays to establish whether miR-9-3p targeted the 3′-UTR of TAZ mRNA. HLF cells transfected with a miR-9-3p mimic significantly suppressed Luc-TAZ-a but not Luc-TAZ-b luciferase activity compared with the control vectors ($P<0.001$). HLF cells transfected with a miR-9-3p mimic did not suppress Luc-TAZ-aM and Luc-TAZ-bM luciferase activity compared with the wild-type 3′-UTR-containing vector. (**C**) Analysis of TAZ expression levels in cells transfected with miR-9-3p mimic and inhibitor by western blotting. TAZ protein levels were reduced in HLF cells transfected with miR-9-3p mimic compared with the controls, and the levels were increased in HuH1 cells treated with miR-9-3p inhibitor. (**D**) miR-9-3p mimic and inhibitor also influenced TAZ localisation. HuH1 cells treated with miR-9-3p inhibitor revealed upregulated TAZ expression and accelerated the nuclear localisation of TAZ. The converse results were confirmed in HLF cells treated with miR-9-3p mimic.

($P<0.01$; Figure 4A). Inversely, HuH1 cells treated with miR-9-3p inhibitor displayed accelerated cell proliferation compared with the control ($P<0.01$; Figure 4A). The expression of p-AKT, p-ERK1/2, and p-β-catenin was decreased by transfection with miR-9-3p mimic. Treatment with miR-9-3p inhibitor increased these expression patterns (Figure 4B). These results indicated that miR-9-3p had a crucial role in cancer cell proliferation via AKT, ERK, and β-catenin signalling in HCC cells.

With regard to cell invasiveness, the protein levels of E- and N-cadherin were not affected by the miR-9-3p mimic and inhibitor (Figure 4C). Cell invasiveness was also not affected by the miR-9-3p mimic and inhibitor (Figure 4D).

DISCUSSION

Although TAZ and YAP are downstream effectors in the Hippo pathway, TAZ is the predominantly expressed protein in HCC cells, suggesting that TAZ appears to be a therapeutic target in HCC. The function of TAZ has become evident in several cancers. For example, TAZ has a critical role in migration, invasion, and tumorigenesis in breast cancer cells (Chan *et al*, 2008). It has been reported that TAZ promotes cell proliferation in lung cancer cells (Zhou *et al*, 2011). Clinically, TAZ overexpression is associated with poor prognosis in breast, lung, and colorectal cancer patients (Yuen *et al*, 2013; Bartucci *et al*, 2014; Noguchi *et al*, 2014). In the present study, we did not found any phenotypical change of cell invasiveness in HCC cells by miR-9-3p mimic and inhibitor. Previously, Chan *et al* (2008) published that TAZ promoted the migration and invasion in breast cancer cells in *Cancer Research*. Guo *et al* (2015) also reported a similar promotion of the same phenotype in HCC cells in *Journal of Cellular Biochemistry*. Although there are many regulators of TAZ expression, miR-9-3p-mediated TAZ expression may participate in cell proliferation, but not in cell invasiveness. Currently, the potential of miRs as anticancer therapeutic targets has been extensively investigated. There are several reports of miRs (such as miR-375 (Liu *et al*, 2010a), -135 (Lin *et al*, 2013), -29 (Tumaneng *et al*, 2012), -let7 (Chaulk *et al*, 2014), and miR-31 (Mitamura *et al*, 2014)) targeting the Hippo pathway, including YAP, which is another downstream effector of the Hippo pathway (Table 2). However, there are no reports of miRs targeting TAZ; this is the first report of a miR that regulates TAZ. TAZ is known to have oncogenic properties in several gastroenterological cancers including HCC (Yuen *et al*, 2013; Han *et al*, 2014). In the present study, overexpression of miR-9-3p using a mimic decreased TAZ expression and resulted in suppressed cell proliferation in HCC. Inversely, inhibition of miR-9-3p induced TAZ expression and promoted proliferation in HCC cells. Thus, miR-9-3p had an onco-suppressive role in HCC cells by downregulating TAZ. These findings suggest that miR-9-3p could be a pharmacological target in HCC.

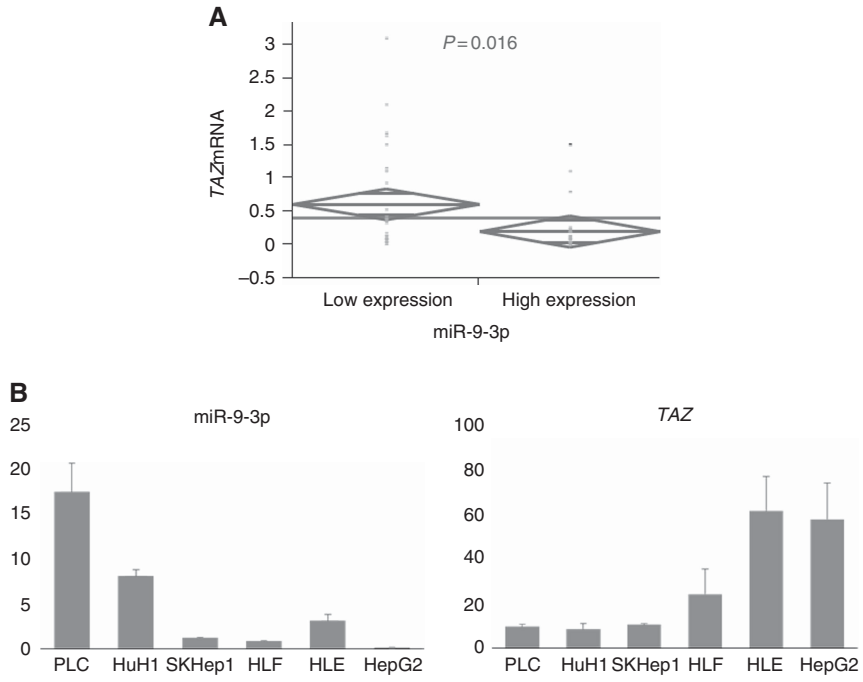

Figure 3. Inverse correlation between miR-9-3p and TAZ mRNA expressions in HCC patients. (**A**) High miR-9-3p expression was significantly associated with low *TAZ* mRNA level in HCC ($P=0.016$). (**B**) There was an inverse correlation between miR-9-3p and TAZ mRNA expressions in HCC cell lines.

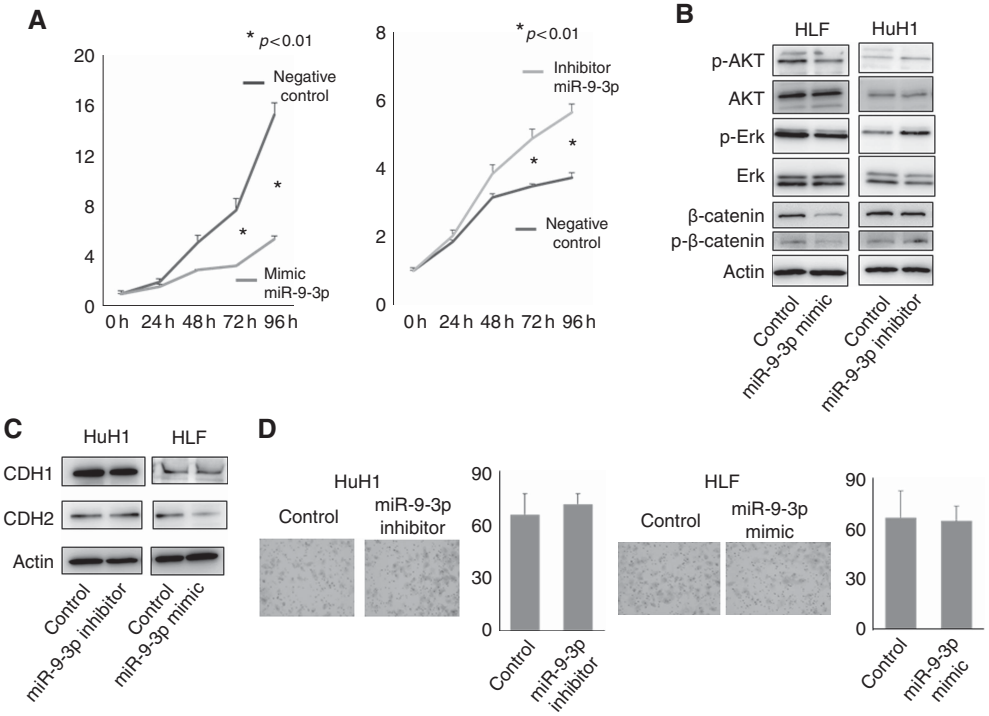

Figure 4. miR-9-3p affects cancer cell proliferation, but not invasiveness. (**A**) Cell proliferation was significantly reduced in HLF cells transfected with miR-9-3p mimics compared with the controls; an inverse result was shown in HuH1 cells treated with miR-9-3p inhibitors ($P<0.01$). (**B**) Phosphorylation of AKT (p-AKT), ERK (p-ERK), and β-catenin (p-β-catenin) was decreased by transfection with miR-9-3p mimic. Treatment with miR-9-3p inhibitor increased these expression. (**C**) The protein levels of E- and N-cadherin were not altered by miR-9-3p mimics and inhibitors. (**D**) Cell invasiveness was not affected by miR-9-3p mimics and inhibitors.

miR-9 is known as a brain-enriched miR. In brain cancer, miR-9 has been mostly reported as an oncogene. However, miR-9 has been also thought to function as both an oncogene and a tumour-suppressor gene. It is overexpressed in brain cancers such as medulloblastoma (Fiaschetti *et al*, 2014) and glioma (Jeon *et al*, 2011). Furthermore, high expression of miR-9

Table 2. The list of microRNAs targeting the Hippo pathway

First author	Journal	Year	MicroRNA	Target gene
Chaulk SG	*J Biol Chem*	2014	miR-let7	YAP
Mitamura T	*Mol Cancer*	2014	miR-31	LATS2
Zhang ZW	*Cell Physiol Biochem*	2013	miR-375	YAP
Lin CW	*Nat Commun*	2013	miR-135b	LATS2
Tumaneng K	*Nat Cell Biol*	2012	miR-29	YAP
Present study			miR-9-3p	TAZ

was associated with poor survival in medulloblastoma patients (Adam *et al*, 2010). However, it showed anticancer effects in other cancer types such as breast cancer (Selcuklu *et al*, 2012; Zawistowski *et al*, 2013),oral squamous cell carcinoma (Yu *et al*, 2013), and gastric cancer (Zheng *et al*, 2013). Furthermore, high expression of miR-9 was associated with poor survival in patients with breast cancer (Zhou *et al*, 2012) and medulloblastoma (Adam *et al*, 2010).

We investigated the relationship between miR-9-3p and *TAZ*, and then confirmed the inverse association between miR-9-3p expression and *TAZ* mRNA expression in HCC clinical samples. Although high TAZ protein expression has been reported to be associated with worse prognostic outcome in HCC patients, it was hard to conclude the prognostic significance of miR-9-3p in the present study with the small and limited number of clinical samples (frozen tissues) available. Further study is required to determine the clinical relevance of miR-9-3p in a large number of HCC patients.

In conclusion, we have identified miR-9-3 as a tumour-suppressing miR targeting *TAZ* expression in HCC cells. miR-9-3p has a crucial role in cell proliferation, but not invasion, via AKT, ERK1/2, and β-catenin signalling in HCC cells.

ACKNOWLEDGEMENTS

We thank Mr Keisuke Miyake, Ms Naomi Yokoyama, and Ms Yoko Ogata for their kind support in preparing experiment reagents.

CONFLICT OF INTEREST

The authors declare no conflict of interest.

REFERENCES

Adam R, Frilling A, Elias D, Laurent C, Ramos E, Capussotti L, Poston GJ, Wicherts DA, de Haas RJ, LiverMetSurvey C (2010) Liver resection of colorectal metastases in elderly patients. *Br J Surg* **97**(3): 366–376.

Bartucci M, Dattilo R, Moriconi C, Pagliuca A, Mottolese M, Federici G, Benedetto AD, Todaro M, Stassi G, Sperati F, Amabile MI, Pilozzi E, Patrizii M, Biffoni M, Maugeri-Sacca M, Piccolo S, De Maria R (2014) TAZ is required for metastatic activity and chemoresistance of breast cancer stem cells. *Oncogene* **34**(6): 681–690.

Chan SW, Lim CJ, Guo K, Ng CP, Lee I, Hunziker W, Zeng Q, Hong W (2008) A role for TAZ in migration, invasion, and tumorigenesis of breast cancer cells. *Cancer Res* **68**(8): 2592–2598.

Chaulk SG, Lattanzi VJ, Hiemer SE, Fahlman RP, Varelas X (2014) The Hippo pathway effectors TAZ/YAP regulate dicer expression and microRNA biogenesis through Let-7. *J Biol Chem* **289**(4): 1886–1891.

Chen CZ, Li L, Lodish HF, Bartel DP (2004) MicroRNAs modulate hematopoietic lineage differentiation. *Science* **303**(5654): 83–86.

Chen D, Sun Y, Wei Y, Zhang P, Rezaeian AH, Teruya-Feldstein J, Gupta S, Liang H, Lin HK, Hung MC, Ma L (2012) LIFR is a breast cancer metastasis suppressor upstream of the Hippo-YAP pathway and a prognostic marker. *Nat Med* **18**(10): 1511–1517.

Croce CM, Calin GA (2005) miRNAs, cancer, and stem cell division. *Cell* **122**(1): 6–7.

Fiaschetti G, Abela L, Nonoguchi N, Dubuc AM, Remke M, Boro A, Grunder E, Siler U, Ohgaki H, Taylor MD, Baumgartner M, Shalaby T, Grotzer MA (2014) Epigenetic silencing of miRNA-9 is associated with HES1 oncogenic activity and poor prognosis of medulloblastoma. *Br J Cancer* **110**(3): 636–647.

Forner A, Llovet JM, Bruix J (2012) Hepatocellular carcinoma. *Lancet* **379**(9822): 1245–1255.

Guo Y, Pan Q, Zhang J, Xu X, Liu X, Wang Q, Yi R, Xie X, Yao L, Liu W, Shen L. Functional and Clinical Evidence that TAZ is a Candidate Oncogene in Hepatocellular Carcinoma. *J Cell Biochem*; e-pub ahead of print 3 February 2015; doi:10.1002/jcb.25117.

Han SX, Bai E, Jin GH, He CC, Guo XJ, Wang LJ, Li M, Ying X, Zhu Q (2014) Expression and clinical significance of YAP, TAZ, and AREG in hepatocellular carcinoma. *J Immunol Res* **2014**: 261365.

Huo X, Zhang Q, Liu AM, Tang C, Gong Y, Bian J, Luk JM, Xu Z, Chen J (2013) Overexpression of Yes-associated protein confers doxorubicin resistance in hepatocellullar carcinoma. *Oncol Rep* **29**(2): 840–846.

Jeon HM, Sohn YW, Oh SY, Kim SH, Beck S, Kim S, Kim H (2011) ID4 imparts chemoresistance and cancer stemness to glioma cells by derepressing miR-9*-mediated suppression of SOX2. *Cancer Res* **71**(9): 3410–3421.

Lin CW, Chang YL, Chang YC, Lin JC, Chen CC, Pan SH, Wu CT, Chen HY, Yang SC, Hong TM, Yang PC (2013) MicroRNA-135b promotes lung cancer metastasis by regulating multiple targets in the Hippo pathway and LZTS1. *Nat Commun* **4**: 1877.

Liu AM, Poon RT, Luk JM (2010a) MicroRNA-375 targets Hippo-signaling effector YAP in liver cancer and inhibits tumor properties. *Biochem Biophys Res Commun* **394**(3): 623–627.

Liu X, Sempere LF, Ouyang H, Memoli VA, Andrew AS, Luo Y, Demidenko E, Korc M, Shi W, Preis M, Dragnev KH, Li H, Direnzo J, Bak M, Freemantle SJ, Kauppinen S, Dmitrovsky E (2010b) MicroRNA-31 functions as an oncogenic microRNA in mouse and human lung cancer cells by repressing specific tumor suppressors. *J Clin Invest* **120**(4): 1298–1309.

Ma Y, Yang Y, Wang F, Wei Q, Qin H (2014) Hippo-YAP signaling pathway: A new paradigm for cancer therapy. *Int J Cancer* **14**(1): 96–105.

Mitamura T, Watari H, Wang L, Kanno H, Kitagawa M, Hassan MK, Kimura T, Tanino M, Nishihara H, Tanaka S, Sakuragi N (2014) microRNA 31 functions as an endometrial cancer oncogene by suppressing Hippo tumor suppressor pathway. *Mol Cancer* **13**: 97.

Noguchi S, Saito A, Horie M, Mikami Y, Suzuki HI, Morishita Y, Ohshima M, Abiko Y, Mattsson JS, Konig H, Lohr M, Edlund K, Botling J, Micke P, Nagase T (2014) An integrative analysis of the tumorigenic role of TAZ in human non-small cell lung cancer. *Clin Cancer Res* **20**(17): 4660–4672.

Qin F, Tian J, Zhou D, Chen L (2013) Mst1 and Mst2 kinases: regulations and diseases. *Cell Biosci* **3**(1): 31.

Ramos A, Camargo FD (2012) The Hippo signaling pathway and stem cell biology. *Trends Cell Biol* **22**(7): 339–346.

Selcuklu SD, Donoghue MT, Rehmet K, de Souza Gomes M, Fort A, Kovvuru P, Muniyappa MK, Kerin MJ, Enright AJ, Spillane C (2012) MicroRNA-9 inhibition of cell proliferation and identification of novel miR-9 targets by transcriptome profiling in breast cancer cells. *J Bio Chem* **287**(35): 29516–29528.

Tumaneng K, Schlegelmilch K, Russell RC, Yimlamai D, Basnet H, Mahadevan N, Fitamant J, Bardeesy N, Camargo FD, Guan KL (2012) YAP mediates crosstalk between the Hippo and PI(3)K-TOR pathways by suppressing PTEN via miR-29. *Nat Cell Biol* **14**(12): 1322–1329.

Wu S, Huang J, Dong J, Pan D (2003) hippo encodes a Ste-20 family protein kinase that restricts cell proliferation and promotes apoptosis in conjunction with salvador and warts. *Cell* **114**(4): 445–456.

Xu MZ, Yao TJ, Lee NP, Ng IO, Chan YT, Zender L, Lowe SW, Poon RT, Luk JM (2009) Yes-associated protein is an independent prognostic marker in hepatocellular carcinoma. *Cancer* **115**(19): 4576–4585.

Yu T, Liu K, Wu Y, Fan J, Chen J, Li C, Yang Q, Wang Z (2013) MicroRNA-9 inhibits the proliferation of oral squamous cell carcinoma cells by suppressing expression of CXCR4 via the Wnt/beta-catenin signaling pathway. *Oncogene* **33**(42): 5017–5027.

Yuen HF, McCrudden CM, Huang YH, Tham JM, Zhang X, Zeng Q, Zhang SD, Hong W (2013) TAZ expression as a prognostic indicator in colorectal cancer. *PloS one* **8**(1): e54211.

Zawistowski JS, Nakamura K, Parker JS, Granger DA, Golitz BT, Johnson GL (2013) MicroRNA 9-3p targets beta1 integrin to sensitize claudin-low breast cancer cells to MEK inhibition. *Mol Cell Biol* **33**(11): 2260–2274.

Zhao B, Li L, Wang L, Wang CY, Yu J, Guan KL (2012) Cell detachment activates the Hippo pathway via cytoskeleton reorganization to induce anoikis. *Genes Dev* **26**(1): 54–68.

Zhao B, Wei X, Li W, Udan RS, Yang Q, Kim J, Xie J, Ikenoue T, Yu J, Li L, Zheng P, Ye K, Chinnaiyan A, Halder G, Lai ZC, Guan KL (2007) Inactivation of YAP oncoprotein by the Hippo pathway is involved in cell contact inhibition and tissue growth control. *Genes Dev* **21**(21): 2747–2761.

Zheng L, Qi T, Yang D, Qi M, Li D, Xiang X, Huang K, Tong Q (2013) microRNA-9 suppresses the proliferation, invasion and metastasis of gastric cancer cells through targeting cyclin D1 and Ets1. *PloS One* **8**(1): e55719.

Zhou X, Marian C, Makambi KH, Kosti O, Kallakury BV, Loffredo CA, Zheng YL (2012) MicroRNA-9 as potential biomarker for breast cancer local recurrence and tumor estrogen receptor status. *PloS One* **7**(6): e39011.

Zhou Z, Hao Y, Liu N, Raptis L, Tsao MS, Yang X (2011) TAZ is a novel oncogene in non-small cell lung cancer. *Oncogene* **30**(18): 2181–2186.

Supplementary Information accompanies this paper on British Journal of Cancer website (http://www.nature.com/bjc)